

## THE EFFECT OF DIE HALF ANGLE IN TUBE NOSING WITH RELIEVED DIE

MITSUMASA ABE, TAKASHI.KUBOKI

University of Electro-Communications (UEC)  
East Building 4-530  
Chofugaoka, 1-5-1 Tokyo, Japan  
E-mail: abe@mce.uec.ac.jp

**Key words:** Tube Forming, Nosing, Relieved Die, Forming Process, FEM.

**Abstract.** This research concentrates on rotary nosing using cone shape dies, in particular using “relieved dies”. “Relieved die” is a cone-shape die with contact surfaces and ground-down relieved surfaces. The objective of this research is to improve the forming limit by reducing the necessary force during the process. The present research focuses attention on the effect of die half angle. Die half angle is important parameter because the angle of nosing depends on the angle of the die in press and rotary nosing. According to the previous research, the forming limit is highest when the number of contact areas is three [1]. Therefore, this paper researched on the effect of die half angle by experiment and calculation, FEM, under the condition that the number of contact areas is three. It is revealed that the optimum contact angle changes depending on the die half angle.

### 1 INTRODUCTION

Various types of metal working process are used to deform pipes and tubes in industrial fields. The tips of drink cans are nosed into a bottle shape so that the caps might be screwed fit to the nosed tips for repeated use. Tubes are also shaped by nosing into vehicle components such as air bags, steering by nosing shaft and so forth [2]. Pipelines for crude oil transportation consist of a number of pipes which are joined together, and the pipes ends are either nosed or expanded in advance. Hydroforming, roll forming, bending, drawing, extrusion and nosing are employed to manufacture structural components for vehicles and buildings, pipes for gas transportation and other products. Nosing is one of the most popular among those processes.

There are several numerical and experimental studies on nosing, where the tool design methods are examined [2-3]. However, one of the major concerns of nosing is fracture limit which is determined by the occurrence of defects like wrinkle, buckling, and fracture. There are many research works on this point [4-5]

The forming limit depends on the type of working process. There are mainly two types of nosing processes: one is press nosing and the other is spinning. In the press nosing process, an axisymmetric cone die is used whereby a tube is pushed into the die and the tube tip is deformed into a cone shapes. Although the forming limit is low, productivity is high and

system of the press machine can be made simple.

In the spinning, on the other hand, tools of rolls or bars are used and the tube is incrementally deformed by repeated contact with the tools. The optimization of the tool path enhances the forming limit and can also manufacture an axisymmetric nosed tube [6]. Moreover, electrically heated rolls can boost the forming limit effectively [7]. However, while the forming limit is much higher than that of press nosing, productivity is much lower.

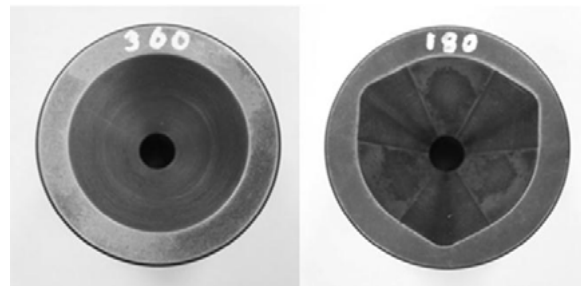
Press nosing and spinning thus have opposite characteristics with regard to the forming limit and productivity. There may be some products which need a little higher forming limit than conventional press nosing. In this case spinning can achieve sufficiently higher forming limit, but the productivity becomes very low. Rotary nosing was proposed as an intermediate method expected to achieve higher forming limit than press nosing and realize higher productivity than spinning [8].

The nosing angle of products depends on that of die. This paper researched on the effect of die half angle by experiment and calculation, FEM. The effect of working surface number and total contact angle was investigated and the optimum conditions attendant upon the die half angle were revealed with emphasis on forming limit.

## 2 ROTARY NOSING WITH RELIEVED DIE

### 2.1 EXPERIMENTAL SETUP

Figures 1 shows the front elevational view of conical die and relieved one. In press nosing, a tube is pushed into the axisymmetric die as shown in Figures 1 [a]. In rotary nosing with relieved die, it is necessary for nosing to rotate a tube or the relieved die because of relief where they are not contact as shown in Figures 1 [b]. Figures 2 shows a schematic illustration of relieved dies. The main parameters of relieved dies are number of working surfaces  $N$ , die half angle  $\alpha$ , total contact area  $\beta$ .



[a] Conical die

[b] Relieved die

**Figure 1:** Comparison of die shapes

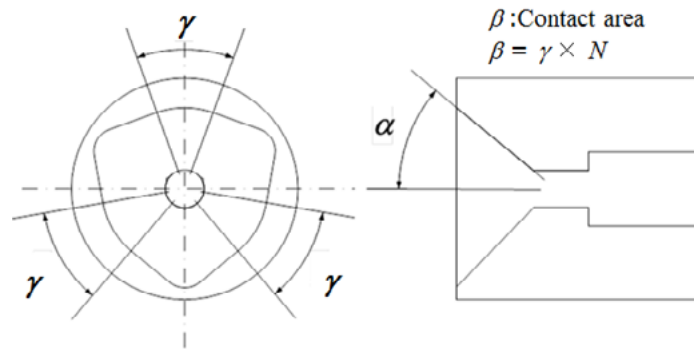


**Figure 2:** Dimension of die

Table 1 shows the condition of experiments and analyses. According to the previous research, the forming limit is highest when the number of contact areas  $N$  is fixed as 3 surfaces. Therefore the number of working surfaces was selected as 3 [1]. The die half angle  $\alpha$  was 30, 40, and 50 degrees. The total contact area  $\beta$  was chose every 60 degrees between 0 and 360 degrees. A lathe was used for rotation of the tube and the tool stand push the relieved die towards the rotated tube. The material of tubes is aluminium alloy A6063. The lubricant for rotary nosing was press oil designed specially for metal working of aluminium. Table 2 shows properties for the alminium alloy 6063. The stress-strain diagram was obtained by tension test. These values of stress and strain were used for finite element analysis. The stress and strain relationship after uniform elongation was calculated by extrapolation. Commonly used elastic constants of aluminium were selected for Young's modulus  $E$  and Poisson's ratio  $\nu$ .

**Table 1:** Nosing condition

Working condition	Number of working surfaces $N$	3
	Half angle $\alpha$ /deg.	30 - 50
	Total contact area $\beta$ /deg.	0 - 360
	Numver of revolution $N$ /rpm	140
	Feed $f$ /mm·rev <sup>-1</sup>	0.1
Tube	Manterial	A6063
	Diameter $D_0$ /mm	30
	Thickness $t_0$ /mm	0.5
	Length for hollow part $L_w$ /mm	30

**Table2:** Mechanical properties of aluminium alloy 6063

Elastic properties	Young's Modulus $E$ /Mpa						70500	
	Poisson's ratio $\nu$						0.34	
Plastic strain	0	0.02	0.04	0.06	0.08	0.1	0.14	0.18
Uni-axial stress	126	156	174	188	200	209	226	239

## 2.1 FEM MODEL SETUP

Elastic-plastic analysis was carried out using the commercial code ELFEN [9], which was developed by Rockfield Software Limited, Swanasea. A von Mises' yield criterion was adopted, and the normality principle was applied to the flow rule. Constrains were dealt with by the penalty function method.

An explicit scheme was used for rotary nosing to shorten the calculation time in the three-dimensional model. While the tube was rotated in the experiments, the die was rotated in analyses in order to shorten calculation time. As tube temperature was low in the experiment, friction heat would be small, and the temperature change was neglected in analyses. Table 4 shows the conditions for finite element analyses. Solid elements were adopted.

Examples of models in the finite element analyses are shown in figure 3 and 4. Analyses was used to check the deformation, and stress and strain history during nosing. For observation about the difference between die half angle, analyses was used to check the round history of stress and strain when the radius of tube tip was around 14 mm.

**Table 3:** Condition for FEM analyses.

Friction coefficient $\mu$		0.25
Mesh division	Thickness	Division number = 4
	Longitude	0.22 -1.1 mm/div
	Hoop	Division number = 64
Analyses scheme		3D dynamic explicit
Element type		Solid

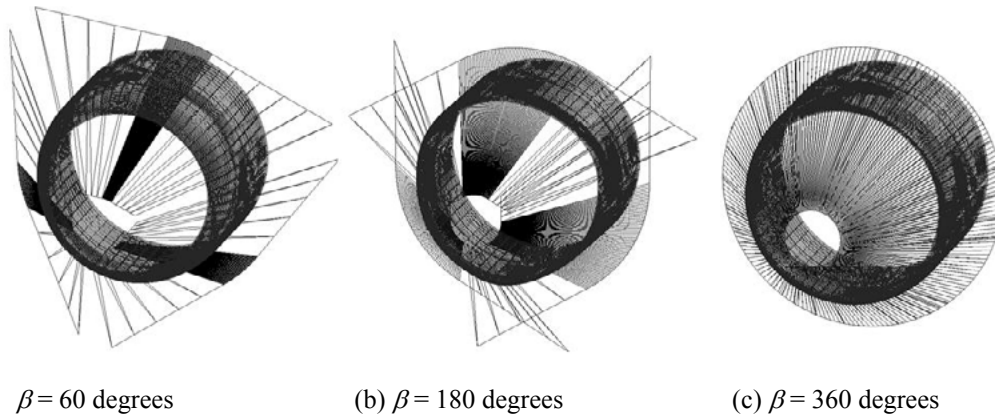
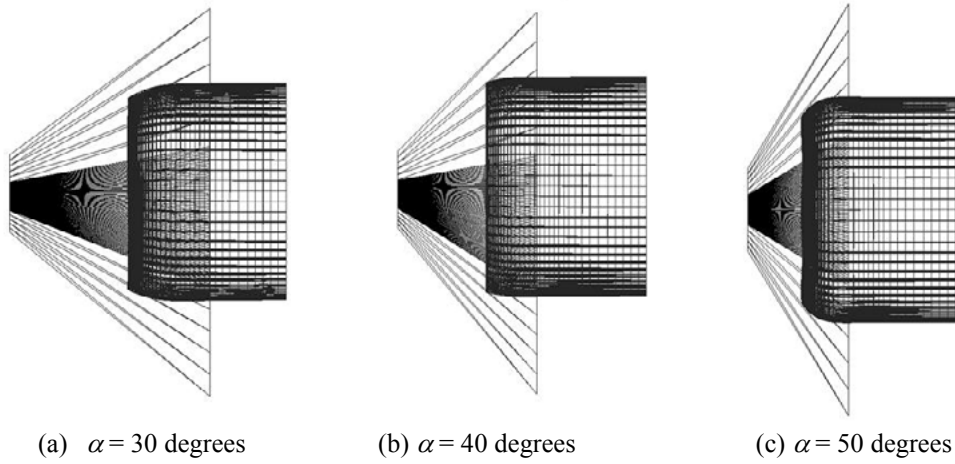


**Figure 3:** FEM Model (die half angle  $\alpha=30$  degree)



### 3 RESULTS

#### 3.1 Forming limit

Figure 5 shows the forming limit experimentally obtained, which is expressed by limit nosing ratio  $\kappa$  defined by the following equation:

$$\kappa = \frac{D_0 - D_L}{D_0} \quad (1)$$

Where,  $D_0$  = Initial diameter, and  $D_L$  = Diameter of tube tip at nosing limit.

The forming limit is highest when die half angle  $\alpha$  is 30, and 40 degrees, and when total contact area  $\beta$  is 240 degrees. However, in the condition that the die half angle  $\alpha$  is 50 degrees, the forming limit is highest when the total contact area  $\beta$  is 180 degrees.

There were three types of defects experimentally observed, of which illustrations are shown in Figure 6. These defects were wrinkle, buckling and split. Table 4 shows the defect mode in experiments. Wrinkle occurs when total contact area  $\beta$  is small and buckling occurs when the total contact area  $\gamma$  is around 180 degrees. However, there was no buckling when the die half angle  $\alpha$  is 30 degrees. Split occurs when total contact area  $\gamma$  is large.

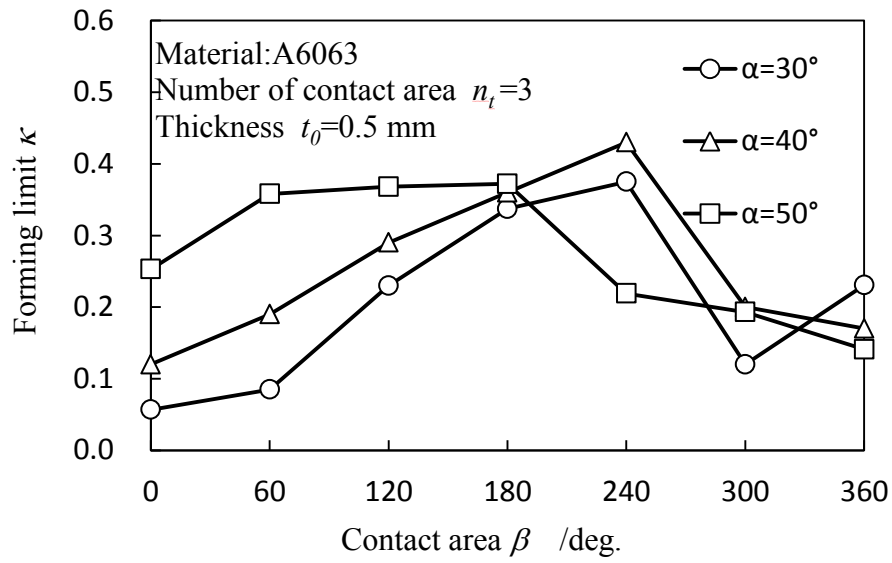


Figure 5: Forming limit in experiments.

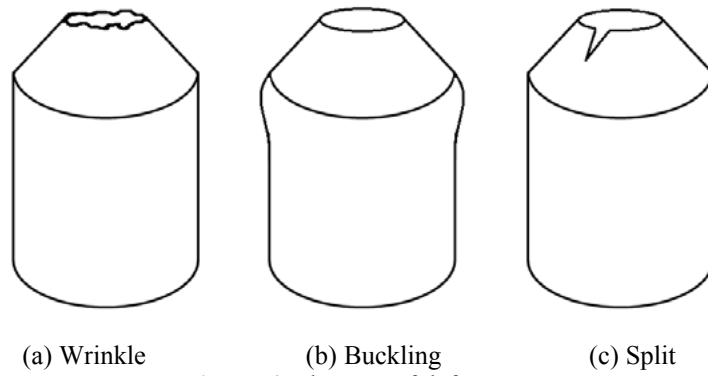


Figure 6: The type of defects.

Table 4: Defect in experiments.

Material : A6063 Surface $N$ : 3		Die half angle $\alpha$ [degrees]		
		30	40	50
Total contact area $\beta$ [degrees]	0	Split	Split	Split
	60	Split	Split	Split
	120	Split	Buckling	Buckling
	180	Split	Buckling	Buckling
	240	Wrinkle	Buckling	Wrinkle
	300	Wrinkle	Wrinkle	Wrinkle
	360	Wrinkle	Wrinkle	Wrinkle

### 3.2 Examination of Mechanism by FEM

FE analyses were used to check the deformation and history of radius, stress and strain. Deformation and radius history, stress-strain history were checked at the tip of the tube as shown in Figure 7. These points,  $P_1$  on the inside surface,  $P_M$  in the middle of the thickness and  $P_X$  on the outside surface were chosen as representative points. Figure 8 shows the examples of analytical results of radius history at outside-surface point  $P_X$  during nosing when the radius is around 14 mm. The rows mean the total contact area  $\beta$ , and columns mean the die half angle  $\alpha$ . The radius history can explain the causes of defect mode. As the total contact area  $\beta$  is small where the defect mode is split, the graph of radius history is undulant shape. As the total contact area  $\beta$  is 180~240 degrees where is optimum condition, the radius passingly increase at relief. As the total contact area is large where the defect mode is wrinkle, the effect of relief is small. Figure 8 (a), (b) and (c) shows the radius history at the total contact area  $\beta = 60$  degrees. Figure 8 (d), (e) and (f) shows the history of radius at the total contact area  $\beta$  is 180 degrees. Figure 8 (f) is the optimum condition at die half angle  $\alpha = 50$  degrees and total contact area  $\beta = 180$  degrees. Figure 8 (g), (h) and (i) shows the history of radius at the total contact area  $\beta = 240$  degrees. Figure 8 (g) and (h) is the optimum condition at die half angle  $\alpha = 30$  and 40 degrees and total contact area  $\beta = 240$  degrees. Figure 8 (j), (k) and (l) shows the examples of analytical results of radius history when the total contact area  $\beta$  is 300 degrees. Figure 8 (j), (k) and (l) shows the examples of analytical results of radius history when the total contact area  $\beta$  is 300 degrees.

Split occurs at the condition in Figure 8 (a), (b), (c) and (d). It is because the radius changes sharply in waves. Regional work hardening happens because of increase of hoop deformation for reducing radius by feed. The buckling occurs at the condition in figure (f), (h) and (i). The radius rises at relieves. The effect of relief is shown to be of benefit at the condition for total contact area = 180~240 degrees. The forming limit is highest at the condition for total contact area = 180~240 degrees where buckling likely occurs except the condition for the die half angle  $\alpha = 30$  degrees. As can be seen from Figure 8 (g), the effect of relief is small when die half angle is 30 degrees compared with the other die half angle conditions. Wrinkle occurs at the condition in figure 8 (g), (i), (j), (k) and (l). If the increase of radius at relief is so small, the effect of relief is small. Figure 9 shows the radius difference  $\Delta r$  when the radius is around 14 mm. The radius difference is defined by the following equation.

$$\Delta r = r_{max} - r_{min} \quad (2)$$

Where,  $r_{max}$  is the maximum radius, and  $r_{min}$  is the minimum radius when the radius is around 14 mm. It is considered the radius difference is so small which causes the effect of relief to become small.

Thus, The radius history can explain the causes of defect mode. As the total contact area  $\beta$  is small, split occurs because of the decrease or increase in radius is sharp. The temporal radius increase at relief is effective for suppression of split and wrinkle at the optimum condition for the total contact area  $\beta = 180\sim 240$  degrees. As the total contact area  $\beta$  is large, wrinkle occurs because the effect of relief is small.

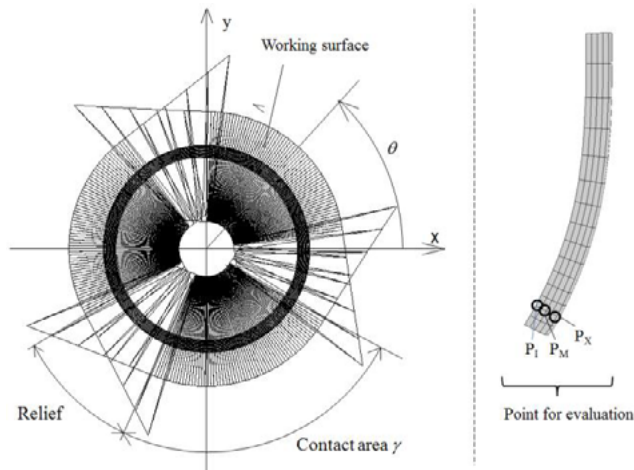


Figure 7: Evaluation points.

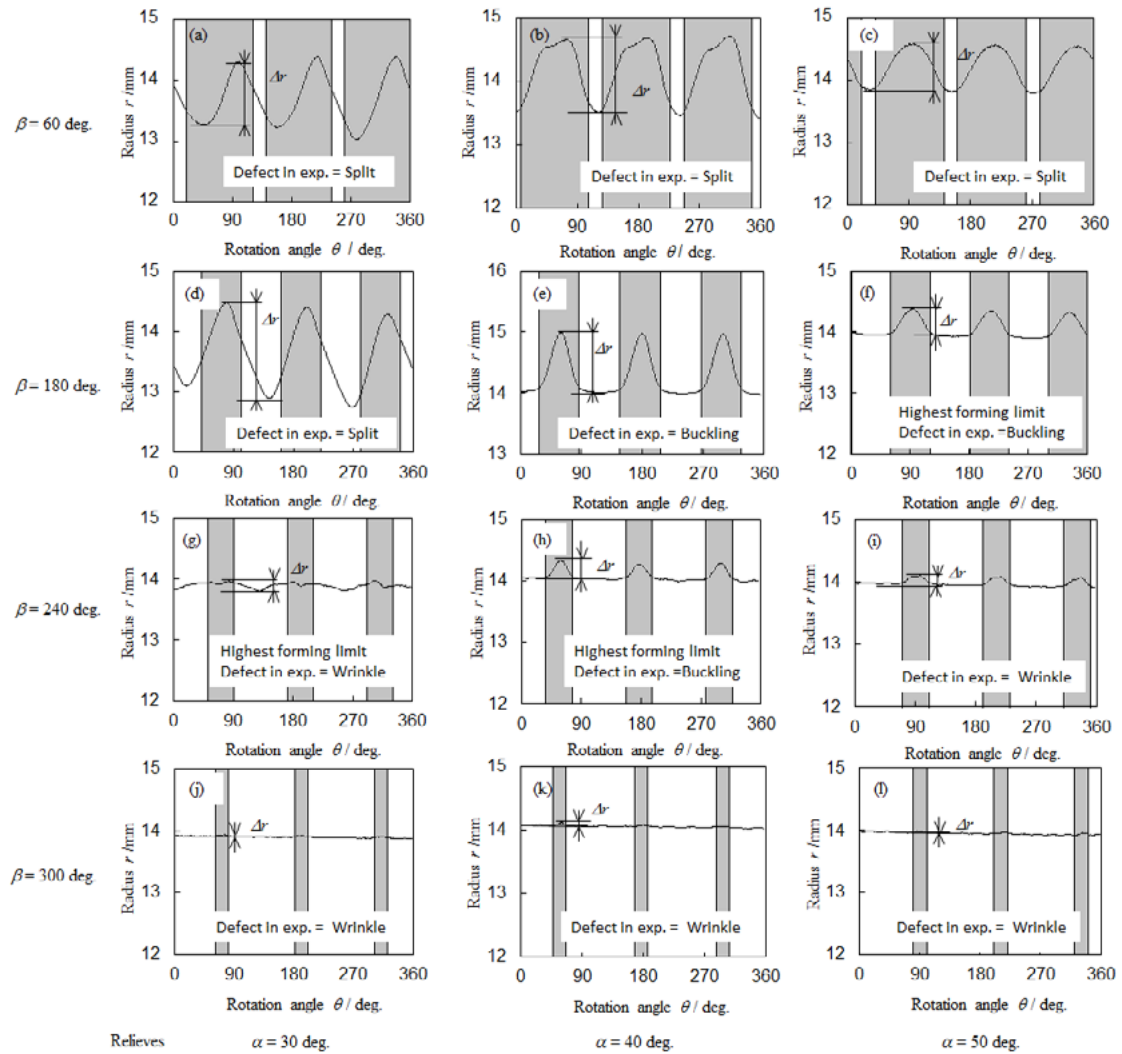
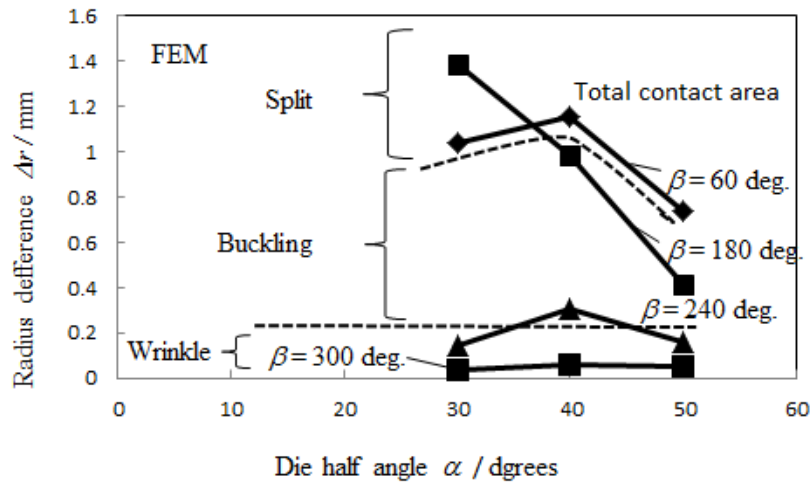


Figure 8: radius history.



Figure 9. Radius Difference  $\Delta r$ 

The optimum condition at die half angle  $\alpha = 30$  and  $40$  degrees is highest when total contact area  $\beta = 240$ . On the other hand, that at die half angle  $\alpha = 50$  degrees is highest when the total contact area  $\beta = 180$  degrees. The hoop stress at total contact area  $\beta = 240$  degrees account for the cause of this phenomenon. Figure 10 shows the examples of analytical results of hoop stress ratio history at evaluation points during nosing when the total contact area  $\beta = 240$  degrees, and the radius is around  $14$  mm. Hoop stress ratio  $s_r$  is defined by the following equation.

$$s_r = \frac{\sigma_\theta}{\sigma_{eq}} \quad (3)$$

Where,  $\sigma_\theta$  = hoop stress,  $\sigma_{eq}$  = deviatoric stress.

As can be seen from the graph in the case of the die half angle is  $50$  degrees, the hoop stress at the inside-surface point  $P_I$  and the middle point  $P_M$  is lower in whole relative to the other conditions. The hoop stress would dominate wrinkle occurrence. Wrinkle occurrence is subjected to a high compressive stress.

Figure 11 shows the average hoop stress at evaluation points  $P_X$ ,  $P_M$  and  $P_I$ , and average of them when the total contact area  $\beta$  is  $240$  degrees. The average of hoop stress  $s_r$  at total contact area  $\beta = 50$  degrees is lower than the other conditions. If the hoop stress is low, tube tip is prestressed. Wrinkle occurs because of high compressive stress at tube tip. This is why the optimum condition at the die half angle  $\alpha = 50$  degrees and contact area  $\beta = 240$  degrees inferior to the other conditions.

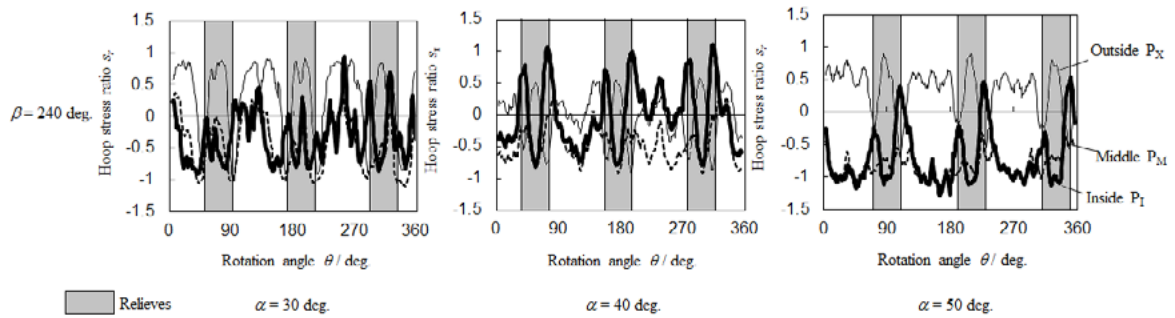


Figure 10: Hoop stress ratio (Total contact area  $\beta = 240$  degrees).

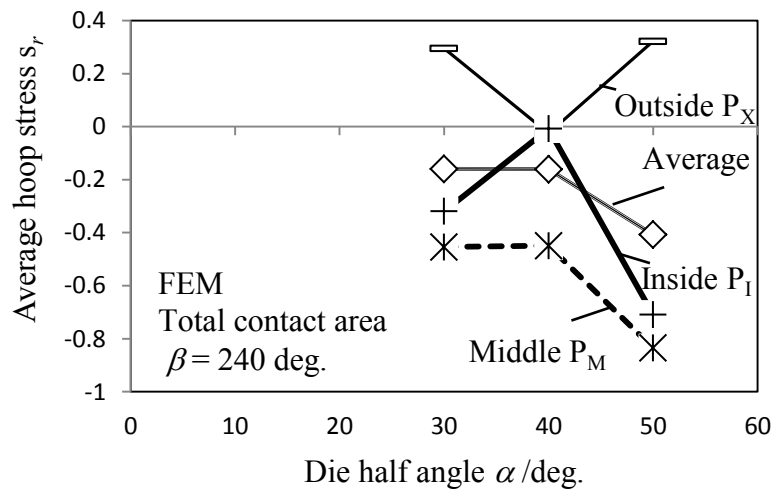


Figure 11: Average hoop stress (Total contact area  $\beta = 240$  degrees).

#### 4 CONCLUSION

- The forming limit of rotary nosing with relieved die is higher than previous rotary nosing although the die half angle changes. The optimum condition is different among the condition of die half angle  $\alpha$ . The radius history proved the effect of relief.
- In the experiment, the optimum condition at die half angle  $\alpha = 30$  and  $40$  degrees is highest when total contact area  $\beta = 240$ . On the other hand, that at die half angle  $\alpha = 50$  degrees is highest when the total contact area  $\beta = 180$  degrees.
- The difference of optimum condition among the die half angle  $\alpha$  is causes the behavior of hoop stress. Compared with the condition for the die half angle  $\alpha = 30$  or  $40$  degrees, hoop stress ratio  $\sigma_r$  is lower at the condition for die half angle  $\alpha = 50$  degrees.

## REFERENCES

- [1] T. Kuboki, A. Kominami, Y. Ohde, M. Murata, Effect of Shape of die on forming limit in rotary nosing with relieved die Steel Res. Int., 2008, Vol.79, pp. 137-144.
- [2] T. Kuboki, A. Kominami, M. Murata, T. Shimoda: Tool design for suppressing fracture at the tip of tube after nosing with die, Computational Plasticity / COMPLAS 8th, Barcelona, September(2005), 599-602
- [3] J. J. Park, N. Rebelo, S. Kobayashi: A new approach to preform design in metal forming with finite element method, Int J. Mach. Tool Des. Res., 23, 1(1984), 71-79.
- [4] K. Manabe, H. Nishimura: Forming loads and forming limits in conical nosing of tubes, J. of Japan Society of Technol. for Plasticity, 23, 225(1966), 335-342, in Japanese
- [5] A. Fatnassi, Y. Tomita, A. Shindo: Non-axisymmetric buckling axisymmetric buckling behavior of elastic-plastic circulation tubes subjected to a nosing operation, Int. J Mech. Sci., 27, 10(1985), 643-651
- [6] T. Irie: Method for forming end part of work, Japan patent, Publication Number 2002-205124.
- [7] M. Murata, T. Kuboki, T. Murai: Compression spinning of circular magnesium tube using heated roller tool, J. Mater. Processing Technol., 162-163(2005), 492-497.
- [8] K. Kitazawa, M. Kobayashi, H. Maruno: Forming limit of flaring and nosing of circular aluminum tube by orbitally rotary forming, J. of Japan Society of Technol. for Plasticity, 30, 344(1989), 1259-1266, in Japanese.
- [9] P. Mullet, J. Rance, "Applied discrete element technology, "Bench Mark, 1 (2003), 17-24.